Front. Phys. 12(3), 128904 (2017)
DOI 10.1007/s11467-017-0656-z

RESEARCH ARTICLE

Diversity of chimera-like patterns from a model of 2D arrays of neurons with nonlocal coupling

Chang-Hai Tian[1,2], Xi-Yun Zhang[1], Zhen-Hua Wang[1], Zong-Hua Liu[1,†]

[1] *Department of Physics, East China Normal University, Shanghai 200062, China*
[2] *School of Data Science, Tongren University, Tongren 554300, China*
Corresponding author. E-mail: †zhliu@phy.ecnu.edu.cn
Received October 19, 2016; accepted December 30, 2016

Chimera states have been studied in 1D arrays, and a variety of different chimera states have been found using different models. Research has recently been extended to 2D arrays but only to phase models of them. Here, we extend it to a nonphase model of 2D arrays of neurons and focus on the influence of nonlocal coupling. Using extensive numerical simulations, we find, surprisingly, that this system can show most types of previously observed chimera states, in contrast to previous models, where only one or a few types of chimera states can be observed in each model. We also find that this model can show some special chimera-like patterns such as gridding and multicolumn patterns, which were previously observed only in phase models. Further, we present an effective approach, i.e., removing some of the coupling links, to generate heterogeneous coupling, which results in diverse chimera-like patterns and even induces transformations from one chimera-like pattern to another.

Keywords chimera state, FitzHugh–Nagumo model, heterogeneous couplings

PACS numbers 89.75.-k, 05.45.Xt

1 Introduction

It is generally believed that the collective behavior of coupled identical oscillators will be either synchronized or unsynchronized for local or global coupling. However, in 2002, Kuramoto and his colleagues noticed that it is also possible to observe peculiar patterns in which the oscillators separate sharply into two groups, one composed of mutually synchronized oscillators with a unique frequency and the other composed of desynchronized oscillators with distributed frequencies, provided that nonlocal coupling is adopted [1]. The surprising aspect of this phenomenon is that it was detected in systems of identical oscillators coupled in a symmetric ring topology with a symmetric interaction function, and it coexists with a completely synchronized state. This highly counterintuitive phenomenon was then given the name chimera state (CS) in 2004 by Abrams and Strogatz [2]. Since then, CSs have been the focus of extensive research in a wide number of models, including neuronal systems [3–6], chaotic oscillators [7, 8], high-dimensional systems [9–13], and even experimental systems [14–16]. To date, CSs can be considered as a variety of self-organized spatiotemporal patterns in which regions of coherence and incoherence coexist. These patterns include the multicluster CS [3, 17], breathing CS [18, 19], spiral wave CS [10, 12, 13, 20–22], circular spot CS and stripe CS [10, 11], traveling CS [23], and chimera death [24–26]. CS is applied in many realistic systems such as the unihemispheric sleep observed in birds, lizards, and dolphins [19, 27, 28]; electrical spiral and scroll waves in the context of the heart [29]; and epileptic seizures [30].

In light of the above results, an important question becomes, "What is the next key topic in the study of CSs?" To identify this topic, we carefully recheck the above results and find three common points: (i) Most of the studies are focused on 1D arrays and consider both phase models and nonphase models, such as the complex Ginzburg–Landau equation and neurons. (ii) A few studies have extended the phenomenon of the CS to 2D arrays, but only in phase models such as Kuramoto oscillators. Further, (iii) each model can show only one or a few types of CS patterns. From these three features, two interesting questions arise. The first is whether it is pos-

*Special Topic: Soft-Matter Physics and Complex Systems (Ed. Zhi-Gang Zheng). arXiv: 1701.05671.

sible to extend the CS to 2D systems of nonphase models, and the second is whether it is possible to use only one system to show most of the observed CS patterns. In fact, the second question is especially important, as the synchronized or partially synchronized patterns in neural systems are closely related to the functions of the brain, such as cognitive and memory functions [31–40]. If we can provide evidence proving that it is possible for one neural system to show most of the CS patterns observed to date, it will be extremely helpful for understanding the large capacity of human memory patterns, which has been understood only in terms of artificial neural networks [41]. It is, therefore, of fundamental importance to construct a model to implement the various CS or similar patterns, collectively referred to as chimera-like patterns, which is the aim of this work. We here propose such a model of FitzHugh–Nagumo (FHN) neurons to show that the CS can indeed be extended to 2D arrays of nonphase models and that the models do show diverse chimera-like patterns. We also find that this model can show some special chimera-like patterns such as gridding and multicolumn patterns, which were previously observed only in phase models. Further, we present an effective approach to generating heterogeneous coupling, i.e., removing some of the coupling links. We find, surprisingly, that heterogeneous coupling can result in diverse chimera-like patterns and, in particular, can cause transformations from one type of chimera-like pattern to another.

The paper is organized as follows. In Section 2, we present the model of 2D arrays of FHN neurons with nonlocal coupling and introduce the local order parameter to measure their collective behavior. In Section 3, we present two methods of nonlocal coupling to generate diverse local synchronized patterns and the new patterns in our model. In Section 4, we discuss the observed patterns and present our conclusions.

2 Model description

We consider a model of 2D arrays of $N \times N$ nonlocally coupled, identical FHN neurons with a periodic boundary condition (the torus configuration). The system is mathematically described as

$$\begin{aligned}\epsilon\dot{u}_{ij} &= u_{ij} - \frac{u_{ij}^3}{3} - v_{ij} + \frac{c}{B_r(i,j)} \\ &\quad \times \sum_{(k,l)\in B_r(i,j)} [b_{uu}(u_{kl}-u_{ij}) + b_{uv}(v_{kl}-v_{ij})], \\ \dot{v}_{ij} &= u_{ij} + a + \frac{c}{B_r(i,j)} \\ &\quad \times \sum_{(k,l)\in B_r(i,j)} [b_{vu}(u_{kl}-u_{ij}) + b_{vv}(v_{kl}-v_{ij})], \end{aligned} \quad (1)$$

where $i,j = 1,\cdots,N$; u and v are the activator and inhibitor variables, respectively; c is the coupling strength; and $\epsilon > 0$ is a small parameter characterizing a time scale separation, which we fix at $\epsilon = 0.05$ in this paper. Depending upon the threshold parameter a, each individual FHN unit exhibits either oscillatory ($|a| < 1$) or excitable ($|a| > 1$) behavior. We here fix it at $a = 0.5$. Each element is coupled to its neighbors within a finite range r defined as

$$\begin{aligned} B_r(i,j) = \{(k,l) : k \in [i-r, i+r], \\ l \in [j-r, j+r], k \neq i, l \neq j\}. \end{aligned} \quad (2)$$

Thus, the coupling region is a square of side r around site (i,j). From Eqs. (1) and (2), we see that there are $(2r+1)^2 - 1$ coupling links from node ij to the nodes in the coupling region, and they constitute a starlike subnetwork. The entire network of system (1) consists of all the N^2 subnetworks. As in Refs. [3, 4], we consider not only direct $u-u$ and $v-v$ coupling, but also cross-coupling between variables u and v. This feature is modeled by the rotational coupling matrix

$$B = \begin{pmatrix} b_{uu} & b_{uv} \\ b_{vu} & b_{vv} \end{pmatrix} = \begin{pmatrix} \cos\phi & \sin\phi \\ -\sin\phi & \cos\phi \end{pmatrix}, \quad (3)$$

which depends on the coupling phase ϕ. We let ϕ be slightly smaller than $\pi/2$; i.e., $\phi = \frac{\pi}{2} - 0.1$.

To study the collective behaviors of system (1) and investigate the existence of CSs, we introduce two quantities. The first is the average phase velocity, which is defined as

$$\omega_{ij} = \frac{2\pi M_{ij}}{\Delta T} \quad (4)$$

for the ij-th FHN unit, where M_{ij} denotes the firing number of neuron (i,j) in the time period $\Delta T = t_2 - t_1$. We here take $t_1 = 3000$ and $t_2 = 5000$. The second is the local order parameter R_{ij}. To determine R_{ij}, we introduce the complex variable $z_{ij} = u_{ij} + iv_{ij}$. Then, we choose a local region with radius δ, i.e.,

$$Q_\delta(i,j) = \{(k,l) : k \in [i-\delta, i+\delta], l \in [j-\delta, j+\delta]\}, \quad (5)$$

which has an area of $(2\delta+1)^2$. When $\delta = 0$, $Q_\delta(i,j)$ contains only the node (i,j). Comparing Eq. (5) with Eq. (2), we see that $Q_\delta(i,j)$ includes node (i,j), whereas $B_R(i,j)$ does not. Letting

$$Z_{ij} = \frac{1}{(2\delta+1)^2} \sum_{(k,l)\in Q_\delta(i,j)} z_{kl}, \quad (6)$$

the local order parameter R_{ij} can be defined as

$$\langle Z_{ij} \rangle = \frac{1}{\delta t} \int_{t-\delta t}^{t} Z_{ij}(s)\mathrm{d}s \equiv R_{ij} e^{\mathrm{i}\psi_{ij}}, \quad (7)$$

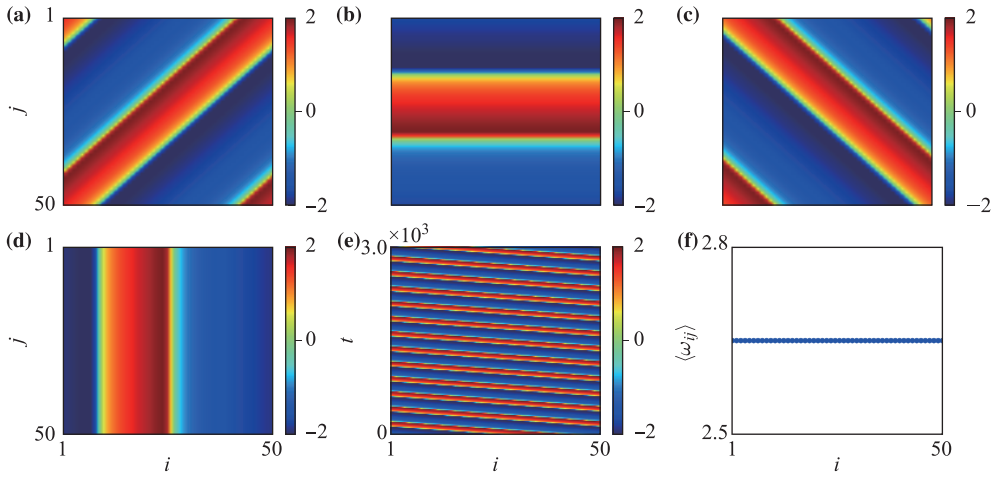

Fig. 1 Traveling patterns. (a, d) The distribution of the variable $u_{ij}(t)$ is plotted on the $i-j$ plane for different parameters. **(a)** Snapshot of the traveling wave along the diagonal with $c = 0.1$, $r = 7$ and $t = 4700$. **(b)** Snapshot of the traveling wave along the j direction with $c = 0.15$, $r = 9$ and $t = 4700$. **(c)** Snapshot of the traveling wave along the clinodiagonal with $c = 0.2$, $r = 7$ and $t = 5000$. **(d)** Snapshot of the traveling wave along the i direction with $c = 0.2$, $r = 10$ and $t = 5000$. **(e)** Traveling wave on the line with $j = 25$ in (d). **(f)** Distribution of the average phase velocity ω_{ij} in (e) with $j = 25$.

with $\delta t = 50$. R_{ij} describes the local average amplitude of the ij-th FHN unit [42, 43]. A larger local order parameter R_{ij} indicates that the ij-th unit belongs to the coherent part of the CS.

3 Numerical simulations

Diversity of chimera-like patterns in the model of 2D arrays of FHN neurons with nonlocal coupling. We numerically simulate the above model of 2D arrays of FHN neurons with nonlocal coupling. In the numerical simulations, we fix $N = 50$ and let the initial conditions be $u_{ij}^2(0) + v_{ij}^2(0) = 4$. By changing the coupling strength c and the coupling radius r, we find that system (1) can show different chimera-like patterns. For example, Figs. 1(a)–(d) show four typical patterns of traveling waves based on the distribution of the variable $u_{ij}(t)$ on the $i - j$ plane, where (a) is a snapshot of the traveling wave along the diagonal with $c = 0.1, r = 7$, and $t = 4700$, (b) is a snapshot of the traveling wave along the j direction with $c = 0.15$, $r = 9$, and $t = 4700$, (c) is a snapshot of the traveling wave along the clinodiagonal with $c = 0.2$, $r = 7$, and $t = 5000$, and (d) is a snapshot of the traveling wave along the i direction with $c = 0.2$, $r = 10$, and $t = 5000$. The traveling behavior can be seen more clearly in Fig. 1(e), which shows the behavior along the line $j = 25$ in Fig. 1(d). We see that the behaviors in Fig. 1(e) are periodic, implying the same average phase velocity ω_{ij} on different i. This conclusion is confirmed in Fig. 1(f) by the distribution of the average phase velocity ω_{ij}.

Figure 2 shows two typical patterns of stripe CSs based on the distribution of ω_{ij} on the $i - j$ plane for (a) $c = 0.1$ and $r = 16$ and (b) $c = 0.15$ and $r = 19$. To see the stripes clearly, Fig. 2(c) shows the evolution of the variable $u_{ij}(t)$ for the line $i = 25$ in Fig. 2(b). We see that the central part is different from its two sides. Figure 2(d) shows the distribution of the average phase velocity $\langle\omega_{ij}\rangle$ in Fig. 2(b) with $i = 25$. It is easy to see that the central part has a distribution of the average phase velocity $\langle\omega_{ij}\rangle$, reflecting the stripes. Similarly, Fig. 3 shows the patterns of a circular spot CS; see its caption for details.

In addition to these typical CS patterns, we find, interestingly, that system (1) can also show special patterns

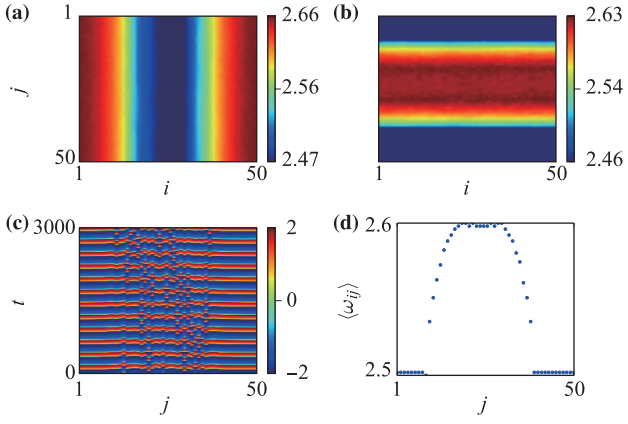

Fig. 2 Stripes chimera states. (a, b) The distribution of ω_{ij} is plotted on the $i-j$ plane for different parameters. **(a)** Case of $c = 0.1$ and $r = 16$. **(b)** Case of $c = 0.15$ and $r = 19$. **(c)** Evolution of the variable $u_{ij}(t)$ for the line with $i = 25$ in (b). **(d)** Distribution of the average phase velocity $\langle\omega_{ij}\rangle$ in (b) with $i = 25$.

such as gridding and multicolumn patterns, which have not been observed in neural systems with both phase and amplitude before. Figure 4 shows typical gridding patterns [(a)–(c)] and multicolumn patterns [(d)–(f)].

To clearly see the diversity of chimera-like patterns, Fig. 5 shows the phase diagram of chimera-like patterns on the $c-r$ plane, where the squares, triangles, circles, crosses, and plus signs represent the traveling, stripe, circular spot, gridding, and multicolumn patterns, respectively. In this plane, empty regions indicate the absence of CS patterns, and overlapping of different symbols indicates that multiple patterns may appear at the same c and r. More patterns may be found outside of this plane, indicating that system (1) can show a variety of chimera-like patterns.

Heterogeneous coupling obtained by removing some of the coupling links. In addition to changing the parameters c and r, there may be other ways to change the coupling scheme that can generate richer and more colorful chimera-like patterns. We here present two such approaches by removing some of the coupling links. The first approach is to remove all the links of node ij within a radius r_c, where $r_c \in [1, r-1]$. That is, we remove all the links of node ij in the range $B_{r_c}(i,j) = \{(k,l) : k \in [i-r_c, i+r_c], l \in [j-r_c, j+r_c], k \neq i, l \neq j\}$ and let the links in the range $B_r(i,j) - B_{r_c}(i,j)$ remain. Figure 6(a) shows the coupling scheme of node ij before the coupling links are removed for $r = 5$. Figure 6(b) shows a schematic illustration of the coupling links for the first approach with $r_c = 2$. We see that the number of coupling links remaining is $(2r+1)^2 - (2r_c+1)^2 = 96$. Once this operation is performed, the coupling matrix will be significantly changed.

We first let the initial conditions and parameters be

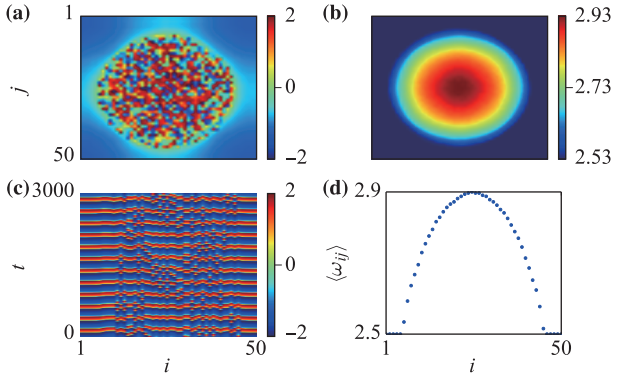

Fig. 3 Circular spots chimera states. **(a)** The distribution of the variable $u_{ij}(t)$ is plotted on the $i-j$ plane for parameters $c = 0.25$ and $r = 16$ where the snapshot of the circular spots is taken at $t = 4500$. **(b)** Distribution of ω_{ij} corresponding to (a). **(c)** Evolution of the variable $u_{ij}(t)$ for the line with $j = 25$ in (a). **(d)** Distribution of the average phase velocity $\langle\omega_{ij}\rangle$ in (b) with $j = 25$.

the same as in Figs. 4(a)–(c) with $r = 12$. We find that the gridding pattern can still be observed when $r_c \in [1, 6]$. Figures 7(a) and (b) show the distributions of ω_{ij} for two typical cases. Comparing them with Fig. 4(c), we see that Fig. 7(b) is similar to Fig. 4(c), but Fig. 7(a) has two more columns than Fig. 4(c), indicating that r_c will influence the structure of the gridding pattern. More interestingly, we find that when $r_c \in [7, 9]$, the gridding pattern is replaced by a pattern of five oval region, as shown in Fig. 7(c), indicating that the gridding pattern has been transformed into a multicircle pattern. Then we let the initial conditions and parameters be the

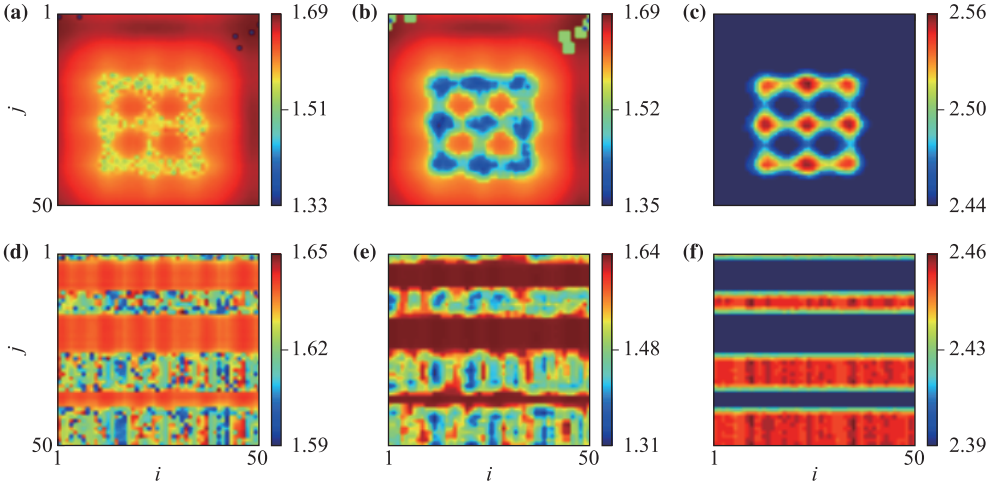

Fig. 4 Typical patterns of gridding and multi-columns. (a–c) denote the case of gridding patterns with $c = 0.3, r = 12$ and $t = 5000$, where **(a)** represents the distribution of R_{ij} for $\delta = 0$; **(b)** the distribution of R_{ij} for $\delta = 1$; and **(c)** the distribution of ω_{ij}. (d–f) denote the case of multi-columns patterns with $c = 0.15, r = 23$ and $t = 5000$, where **(d)** represents the distribution of R_{ij} for $\delta = 0$; **(e)** the distribution of R_{ij} for $\delta = 1$; and **(f)** the distribution of ω_{ij}.

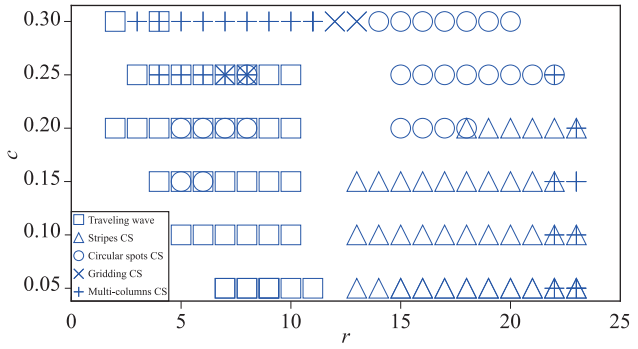

Fig. 5 Phase diagram of chimera-like patterns on the parameters $c-r$ plane. In this plane, the local regions with "symbols" denote the existence of chimera-like patterns and the empty regions imply no chimera-like patterns, where the "squares", "triangles", "circles", "crosses" and "pluses" represent the traveling, stripes, circular spots, gridding and multi-columns patterns, respectively.

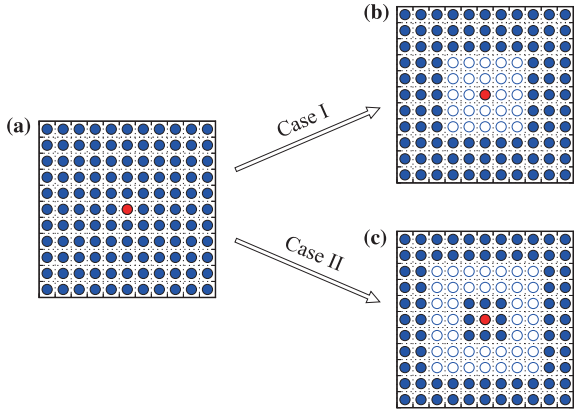

Fig. 6 Schematic illustration of removing part of the coupling links. **(a)** The coupling scheme of node ij before removing part of the coupling links where $r = 5$ and the central "red" site denotes the chosen node-ij. **(b)** The first approach to remove coupling links with $r_c = 2$: remove all the links in the range $B_{r_c}(i,j)$ and let the links in the range $B_r(i,j) - B_{r_c}(i,j)$ be remained. That is, the links between the "red" node and "white" nodes are removed, while the links between the "red" node and "blue" nodes are remained. **(c)** The second approach to remove links: The parameters are chosen as $r = 5$ and $m = 2$, which gives $r_m = [2,3]$. Thus, we remove all the middle links within the circles 2 and 3 and let the links on the first, fourth and fifth circles be remained.

same as in Figs. 4(d)–(f) with $r = 23$. We find that we can still observe the pattern of three columns when $r_c \in [1,2]U[9,15]$. Figure 7(d) shows such a typical result with $r_c = 15$. However, we observe a pattern of five columns when $r_c \in [3]U[5,8]U[16,18]$ and a pattern of seven columns when $r_c \in [4]U[19,20]$. Figures 7(e) and (f) show typical results for $r_c = 17$ and 19, respectively.

We observed similar results for other cases such as the traveling wave, stripes, and circular spots and found that their patterns differ greatly from those in Figs. 1, 2, and 3, respectively, confirming the diversity of chimera-like patterns.

The second approach is to remove all the coupling links in the middle of a specific range but keep at least the nearest and farthest coupling links. Specifically, we let m be the number of removed circles and let $m \in [1, r-2]$, which determines how many circles of coupling links will be removed. In this sense, the coupling links within the radius $r_m = [int(r/2) + 1 - int(m/2), int(r/2) + 1 + int((m-1)/2))]$ will be removed. Figure 6(c) illustrates schematically the coupling links for the second approach with $r = 5$ and $m = 2$. We see that the remaining links are in two separate regions, and the removed links are in the range of $r_m = [2,3]$, indicating that all the links in circles 2 and 3 are removed. This approach makes the coupling matrix more heterogeneous, in contrast to the first approach.

To see how changing the coupling matrix influences the chimera-like patterns, we first let the initial conditions and parameters be the same as those in Figs. 4(a)–(c) with $r = 12$. We use the second approach to remove coupling links and find that the gridding pattern can still be observed when $m \leq 2$. Figures 8(a) and (b) show the distributions of ω_{ij} for $m = 1$ and 2, respectively. We see that they are similar to those in Fig. 4(c). However, we find that when $m = 8$, the gridding pattern is replaced by a pattern of four oval region, as shown in Fig. 8(c). Then we let the initial conditions and parameters be the same as those in Figs. 4(d)–(f) with $r = 23$. We find that we can still observe the pattern of three columns when $m \leq 8$. However, we observe a pattern of two columns when $m \in [15,17]$; the coexistence of a circular spot and a stripe when $m = 9, 11, 13, 14$; two stripes when $m = 10$ and 12; and a pattern of seven columns when $m = 18$. Figures 8(d)–(f) show the typical results for $m = 14, 15$, and 18, respectively. We can also compare each panel in Fig. 8 with the corresponding panel in Fig. 7. We easily see that the panels in the two figures are different, indicating the diversity of the chimera-like patterns.

We observed similar results for other cases such as the traveling wave, stripes, and circular spots using this approach, again confirming the diversity of patterns.

4 Discussion and conclusions

The networked neural model in Eq. (1) is in fact not a phase model. Compared with phase models, it contains more information, including both the aspect from phase and that from amplitude. In this sense, much more information will be transmitted by the coupling links than in a purely phase model, and thus the system will be

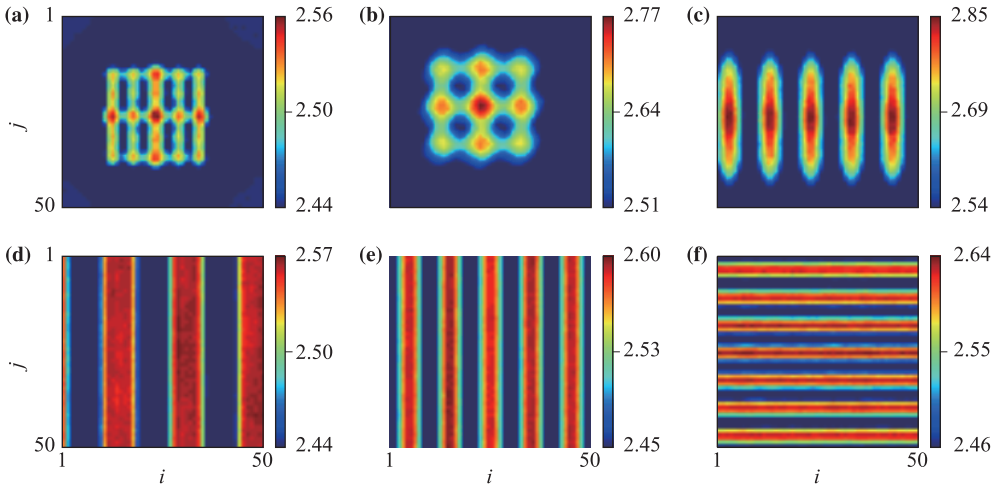

Fig. 7 Typical patterns of gridding and multi-columns for the first approach to remove part of the coupling links. (a–f) represent the distributions of ω_{ij} for different parameters. (a–c) have the same initial conditions and parameters with that in Figs. 4(a)–(c) with $r = 12$. The parameter r_c is chosen as $r_c = 3$ in **(a)**, $r_c = 6$ in **(b)**, and $r_c = 7$ in **(c)**. (d–f) have the same initial conditions and parameters with that in Figs. 4(d)–(f) with $r = 23$. The parameter r_c is chosen as $r_c = 15$ in **(d)**, $r_c = 17$ in **(e)**, and $r_c = 19$ in **(f)**.

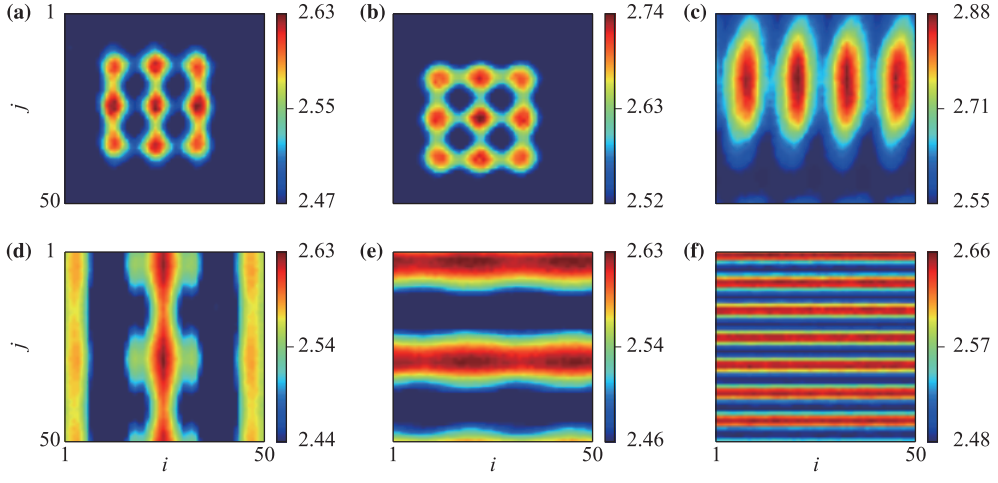

Fig. 8 Typical patterns of gridding and multi-columns for the second approach to remove coupling links. (a–f) represent the distributions of ω_{ij} for different parameters. (a–c) have the same initial conditions and parameters with that in Figs. 4(a)–(c) with $r = 12$. The parameter m is chosen as $m = 1$ in **(a)**, $m = 2$ in **(b)**, and $m = 8$ in **(c)**. (d–f) have the same initial conditions and parameters with that in Figs. 4(d)–(f) with $r = 23$. The parameter m is chosen as $m = 14$ in **(d)**, $m = 15$ in **(e)**, and $m = 18$ in **(f)**.

able to show a richer variety of behavior, which is the main reason for the diversity of chimera-like patterns in a single networked neural system.

A characteristic feature of Eq. (1) is its nonlocal coupling, which is fundamentally different from both global coupling and nearest-neighbor coupling. Global coupling generally induces global synchronization that is robust to slight changes in the network structure. In contrast, nearest-neighbor coupling does not easily result in global synchronization unless a sufficiently large coupling strength is used. Nonlocal coupling falls between these two extremes. Thus, it cannot cause global synchronization but can only sustain local synchronization, which guarantees the existence of different chimera-like patterns.

More importantly, we present a new way of changing the structure of coupling links, which is the guarantee of the diversity of the chimera-like patterns. Unlike the use of homogeneously nonlocal coupling in a region of radius r, removing some of the coupling links yields heterogeneously nonlocal coupling and provides more possible coupling structures, greatly increasing the diversity

of the chimera-like patterns. On the other hand, this idea can be easily extended to different schemes. Notice that in both cases I and II in Fig. 6, the number of coupling links remains identical for each node. Therefore, an easy way to extend them is to design irregular coupling schemes in which the number of coupling links may be different for different nodes. For example, we may randomly remove some of the coupling links. In particular, we may also remove the coupling links on purpose so that the final coupling networks can meet desired criteria, such as scale-free networks or other complex networks. In this way, we may expect new chimera-like patterns.

In conclusion, we observed diverse chimera-like patterns in 2D arrays of FHN neurons with nonlocal coupling, which were previously observed only in 1D arrays or 2D arrays in phase models. The numbers of both coupling schemes and the resulting chimera-like patterns were vastly increased by removing some of the coupling links.

Acknowledgements This work was partially supported by the National Natural Science Foundation of China under Grant Nos. 11135001 and 11375066, the National Basic Research Program of China (973 Program) under Grant No. 2013CB834100, the Scientific Research Starting Foundation of Tongren University under Grant No. TS1118, and the Natural Science Foundation of Guizhou Province Education Department under Grant No. KY[2014]316.

References and notes

1. Y. Kuramoto and D. Battogtokh, Coexistence of coherence and incoherence in nonlocally coupled phase oscillators, *Nonlinear Phenom. Complex Syst.* 5, 380 (2002)
2. D. M. Abrams and S. H. Strogatz, Chimera states for coupled oscillators, *Phys. Rev. Lett.* 93(17), 174102 (2004)
3. I. Omelchenko, O. E. Omel'chenko, P. Hövel, and E. Schöll, When nonlocal coupling between oscillators becomes stronger: Patched synchrony or multichimera states, *Phys. Rev. Lett.* 110(22), 224101 (2013)
4. J. Hizanidis, V. G. Kanas, A. Bezerianos, and T. Bountis, Chimera states in networks of nonlocally coupled HindmarshRose neuron models, *Inter. J. Bif. Chaos* 24(03), 1450030 (2014)
5. H. Sakaguchi, Instability of synchronized motion in nonlocally coupled neural oscillators, *Phys. Rev. E* 73(3), 031907 (2006)
6. S. Olmi, A. Politi, and A. Torcini, Collective chaos in pulsecoupled neural networks, *Europhys. Lett.* 92(6), 60007 (2010)
7. I. Omelchenko, Y. Maistrenko, P. Hövel, and E. Schöll, Loss of coherence in dynamical networks: Spatial chaos and chimera states, *Phys. Rev. Lett.* 106(23), 234102 (2011)
8. I. Omelchenko, B. Riemenschneider, P. Hövel, Y. Maistrenko, and E. Schöll, Transition from spatial coherence to incoherence in coupled chaotic systems, *Phys. Rev. E* 85(2), 026212 (2012)
9. O. E. Omel'chenko, M. Wolfrum, S. Yanchuk, Y. L. Maistrenko, and O. Sudakov, Stationary patterns of coherence and incoherence in two-dimensional arrays of non-locally-coupled phase oscillators, *Phys. Rev. E* 85(3), 036210 (2012)
10. M. J. Panaggio and D. M. Abrams, Chimera states on a flat torus, *Phys. Rev. Lett.* 110(9), 094102 (2013)
11. M. J. Panaggio and D. M. Abrams, Chimera states on the surface of a sphere, *Phys. Rev. E* 91(2), 022909 (2015)
12. J. Xie, E. Knobloch, and H. C. Kao, Twisted chimera states and multicore spiral chimera states on a two-dimensional torus, *Phys. Rev. E* 92(4), 042921 (2015)
13. Y. Maistrenko, O. Sudakov, O. Osiv, and V. Maistrenko, Chimera states in three dimensions, *New J. Phys.* 17(7), 073037 (2015)
14. A. M. Hagerstrom, T. E. Murphy, R. Roy, P. Hövel, I. Omelchenko, and E. Schöll, Experimental observation of chimeras in coupled-map lattices, *Nat. Phys.* 8(9), 658 (2012)
15. M. R. Tinsley, S. Nkomo, and K. Showalter, Chimera and phasecluster states in populations of coupled chemical oscillators, *Nat. Phys.* 8(9), 662 (2012)
16. E. A. Viktorov, T. Habruseva, S. P. Hegarty, G. Huyet, and B. Kelleher, Coherence and incoherence in an optical comb, *Phys. Rev. Lett.* 112(22), 224101 (2014)
17. N. Yao, Z. G. Huang, C. Grebogi, and Y. C. Lai, Emergence of multicluster chimera states, *Sci. Rep.* 5, 12988 (2015)
18. D. M. Abrams, R. Mirollo, S. H. Strogatz, and D. A. Wiley, Solvable model for chimera states of coupled oscillators, *Phys. Rev. Lett.* 101(8), 084103 (2008)
19. R. Ma, J. Wang, and Z. Liu, Robust features of chimera states and the implementation of alternating chimera states, *Europhys. Lett.* 91(4), 40006 (2010)
20. E. A. Martens, C. R. Laing, and S. H. Strogatz, Solvable model of spiral wave chimeras, *Phys. Rev. Lett.* 104(4), 044101 (2010)
21. C. Gu, G. St-Yves, and J. Davidsen, Spiral wave chimeras in complex oscillatory and chaotic systems, *Phys. Rev. Lett.* 111(13), 134101 (2013)
22. C. R. Laing, The dynamics of chimera states in heterogeneous Kuramoto networks, *Physica D* 238(16), 1569 (2009)
23. J. Xie, E. Knobloch, and H. C. Kao, Multicluster and traveling chimera states in nonlocal phase-coupled oscillators, *Phys. Rev. E* 90(2), 022919 (2014)

24. A. Zakharova, M. Kapeller, and E. Schöll, Chimera death: Symetry breaking in dynamical networks, *Phys. Rev. Lett.* 112(15), 154101 (2014)
25. P. S. Dutta and T. Banerjee, Spatial coexistence of synchronized oscillation and death: A chimeralike state, *Phys. Rev. E* 92(4), 042919 (2015)
26. T. Banerjee, Mean-field-diffusioninduced chimera death state, *Europhys. Lett.* 110(6), 60003 (2015)
27. M. J. Panaggio and D. M. Abrams, Chimera states: Coexistence of coherence and incoherence in networks of coupled oscillators, *Nonlinearity* 28(3), R67 (2015)
28. N. C. Rattenborg, C. J. Amlaner, and S. L. Lima, Behavioral, neurophysiological and evolutionary perspectives on unihemispheric sleep, *Neurosci. Biobehav. Rev.* 24(8), 817 (2000)
29. E. M. Cherry and F. H. Fenton, Visualization of spiral and scroll waves in simulated and experimental cardiac tissue, *New J. Phys.* 10(12), 125016 (2008)
30. A. Rothkegel and K. Lehnertz, Irregular macroscopic dynamics due to chimera states in small-world networks of pulse-coupled oscillators, *New J. Phys.* 16(5), 055006 (2014)
31. W. Singer, Neuronal synchrony: A versatile code for the definition of relations? *Neuron* 24(1), 49 (1999)
32. J. F. Hipp, A. K. Engel, and M. Siegel, Oscillatory synchronization in large-scale cortical networks predicts perception, *Neuron* 69(2), 387 (2011)
33. P. R. Roelfsema, A. Engel, P. König, and W. Singer, Visuomotor integration is associated with zero time-lag synchronization among cortical areas, *Nature* 385(6612), 157 (1997)
34. T. P. Vogels and L. F. Abbott, Signal propagation and logic gating in networks of integrate-and-fire neurons, *J. Neurosci.* 25(46), 10786 (2005)
35. A. Aertsen, M. Diesmann, and M.O. Gewaltig, Stable propagation of synchronous spiking in cortical neural networks, *Nature* 402(6761), 529 (1999)
36. T. Womelsdorf, J. M. Schoffelen, R. Oostenveld, W. Singer, R. Desimone, A. K. Engel, and P. Fries, Modulation of neuronal interactions through neuronal synchronization, *Science* 316(5831), 1609 (2007)
37. K. Xu, W. Huang, B. Li, M. Dhamala, and Z. Liu, Controlling self-sustained spiking activity by adding or removing one network link, *Europhys. Lett.* 102(5), 50002 (2013)
38. Z. Liu, Organization network enhanced detection and transmission of phase-locking, *Europhys. Lett.* 100(6), 60002 (2012)
39. J. Wang and Z. Liu, A chain model for signal detection and transmission, *Europhys. Lett.* 102(1), 10003 (2013)
40. K. Xu, X. Zhang, C. Wang, and Z. Liu, A simplified memory network model based on pattern formations, *Sci. Rep.* 4, 7568 (2014)
41. J. Hopfield, Neural networks and physical systems with emergent collective computational abilities, *Proc. Natl. Acad. Sci. USA* 79(8), 2554 (1982)
42. P. C. Matthews, R. E. Mirollo, and S. H. Strogatz, Dynamics of a large system of coupled nonlinear oscillators, *Physica D* 52(2–3), 293 (1991)
43. M. C. Cross, J. L. Rogers, R. Lifshitz, and A. Zumdieck, Synchronization by reactive coupling and nonlinear frequency pulling, *Phys. Rev. E* 73(3), 036205 (2006)